

An investigation into the possibility of measuring an 'X-ray modulus' and new evidence for hexagonal packing in polyacrylonitrile

R. A. Allen and I. M. Ward

IRC in Polymer Science and Technology, University of Leeds, Leeds LS2 9JT, UK

and Z. Bashir*

Courtaulds Research, 72 Lockhurst Lane, Coventry CV6 5RS, UK

(Received 26 May 1993; revised 19 October 1993)

Although the 'crystal modulus' of most semicrystalline polymers has been estimated by measuring the displacement of meridional X-ray reflections on application of a stress to an oriented specimen, this method has not been applied to polyacrylonitrile (PAN). The X-ray diffraction behaviour and the long-range order in PAN are very controversial. Several reports state that the diffraction pattern of oriented PAN contains only equatorial peaks and therefore the material is only laterally ordered. However, there are a few papers that mention or imply sharp meridional and off-axis reflections. We have produced two samples of PAN which were oriented by different production methods. Both our specimens always produced the 'standard' fibre pattern of PAN which consists of just two equatorial peaks and weak, diffuse meridional scattering. The standard pattern has been assumed in the literature to arise from a hexagonal packing of chains with no chain-axis order. One of our specimens had a preferred double orientation of crystallographic axes and when the X-ray beam was passed along the fibre axis of this sample, a six-arc pattern was obtained. This result is new evidence for hexagonal symmetry in a bulk sample of PAN. As we were unable to reproduce the claims made by a few authors regarding sharp meridional peaks, the crystal modulus of PAN could not be measured in the same way as has been done with other polymers. However, by considering the rod-like conformation adopted by the PAN chains, and comparing it with polymers which adopt a helical form, it was estimated that the maximum tensile modulus of atactic PAN would be about 55 GPa.

(Keywords: X-ray modulus; meridional peaks; double orientation)

INTRODUCTION

There are various experimental methods to estimate the maximum axial tensile modulus attainable by polymers. In the case of polyethylene (PE), X-ray methods¹ indicate that the 'crystal modulus' is 240 GPa. Raman studies^{2,3} have led to values of 340 and 358 GPa for the maximum modulus of PE. Theoretical calculations⁴⁻⁶ of varying sophistication have also led to values in the range 182-340 GPa for PE. Unoriented bulk PE in contrast has moduli of <1 GPa. Thus, there was a tremendous drive in the last 10-15 years to exploit the high modulus potential of PE. With the advent of 'gel spinning' of high molecular weight PE, the high stiffness of this polymer has come somewhere near full realization, with values in the range 100-160 GPa being attained⁷.

Dulmage and Contois appear to be the first workers to measure the elastic modulus of the crystalline regions of poly(ethylene terephthalate) using the X-ray method⁸. Sakurada *et al.*^{1,9} extended this to measure the crystal modulus of PE, poly(vinyl alcohol), poly(vinylidene chloride), isotactic polypropylene, polyoxymethylene and cellulose I and II. The technique involves measuring the increase in a meridional spacing on the application of a

stress to an oriented specimen, and with the assumption of a homogeneous stress, translating this to a crystal strain^{1,9}.

There appear to be no experimental or theoretical estimates of the maximum modulus attainable by polyacrylonitrile (PAN). Considering that it is a commercially important polymer, this is surprising. PAN copolymer fibres which are used for textile applications have moduli of ~5-7 GPa, while fibres used as carbon fibre precursor have moduli of ~10 GPa. The highest modulus reported^{10,11} using high molecular weight homopolymer PAN appears to be in the range 30-33 GPa. It is known that the higher the modulus of the PAN precursor, the higher the modulus of the resulting carbon fibre. Hence, it would be interesting to know what the limiting modulus would be for this polymer.

Thus, we sought to see if the maximum modulus of PAN could be estimated by the X-ray method. Initially, it was thought that this would be possible because authors such as Colvin and Storr¹², Hinrichsen and Orth¹³, Kumamaru *et al.*¹⁴ and Stefani *et al.*¹⁵ have reported meridional reflections in oriented PAN. In principle, such reflections would allow the measurement of a crystal modulus.

However, it should be pointed out that the majority of workers¹⁶⁻²⁰ have not observed any strong, sharp

* To whom correspondence should be addressed

meridional peaks in highly oriented PAN. The 'standard' diffraction pattern of oriented PAN consists of just two equatorial peaks with spacings of ~ 0.52 and 0.30 nm, and very weak, diffuse meridional scattering.

When this work was commenced, it was hoped that the meridional reflections reported by Colvin and Storr¹² could be reproduced and used to measure the crystal modulus of PAN.

EXPERIMENTAL

Samples

The first type of sample in this study was made by a casting process. Thin films were cast from a dimethylsulfoxide (DMSO) solution with 10% polymer by weight. Polymers with inherent viscosities of 1.5, 7.85 and 14.8 dl g^{-1} (measured in dimethylformamide at 25°C) were used. These correspond to approximate molecular weights of 60 000, 544 000 and 1 270 000, respectively. After drying the films, there was $< 5\%$ DMSO left in the film. Rectangular strips of these films were drawn to various draw ratios on a hot stage at 110°C .

The second sample was prepared by a non-solvent based process which we shall refer to as 'compression-elongation'. PAN powder obtained from Polysciences ($M_w = 150\,000$) was heated to 135°C and compressed into isotropic plaques under a load of 20×10^3 kg applied to an area of $20 \text{ mm} \times 50 \text{ mm}$. The final sample thickness was between 2 mm and 3 mm, depending on the starting quantity of powder used. To orient the sample, the PAN plaque was sandwiched between two 3 mm thick poly(methyl methacrylate) (PMMA) sheets, and then placed in a mould with a U-shaped lower part and a T-shaped upper part (Figure 1). The mould was heated to 135°C and when the temperature had equilibrated, a load up to 70 000 N was progressively applied. This caused the PAN/PMMA sample length to increase from 50 to 100 mm. The press and sample were then cooled as rapidly as possible (a process taking ~ 15 min) to below 100°C to prevent the PMMA contracting to its original length on removal of the load. After releasing the sample from the mould, the PAN plaque was found to have doubled its length and undergone a reduction in its width and thickness. From pen marks drawn on the sample before processing, an approximate central 50 mm length received a draw ratio of $\sim 3:1$ and the ends a relatively lower draw ratio. The PAN could be easily removed from the outer PMMA layer. After cutting off the ends with lower draw ratio, the process was repeated several times till a sample with a maximum draw ratio of 19:1 was produced.

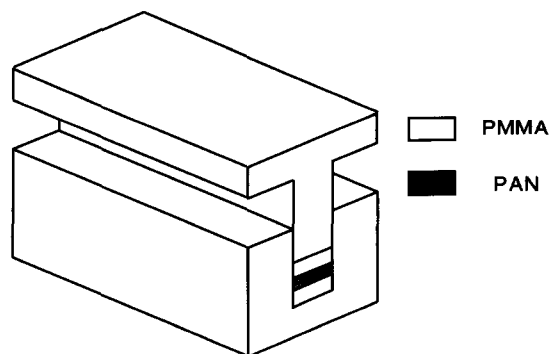


Figure 1 Diagram showing the mould used for making the compression-elongated PAN sample

X-ray examination

X-ray diffraction experiments were performed with Ni-filtered $\text{Cu K}\alpha$ radiation generated by a Hilton-Brooks generator working at 40 kV and 30 mA. Diffractometer scans were obtained with either a Siemens diffractometer or a Huber texture goniometer (model 4020). Data were stored and processed on a computer.

RESULTS AND DISCUSSION

First, we shall discuss the X-ray results obtained with the two types of PAN samples: uniaxially oriented films (cast from DMSO solution and subsequently drawn), and the sample produced by the compression-elongation method. In the process, we shall examine the controversial nature of the long-range order in PAN with particular reference to the work of the few authors who claim to have observed meridional reflections in PAN. Following this, we shall consider the issue of estimating the maximum tensile modulus of PAN, which was the original impetus of the work.

X-ray diffraction patterns of drawn, cast films

These drawn films always showed what we shall call the 'standard' diffraction pattern of oriented PAN. This contains just two equatorial peaks d_1 and d_2 which occur at about $2\theta = 17$ and 29.5° , respectively. This is shown in Figure 2, which is the equatorial diffractogram of a film which was drawn ten times. With this particular drawn film, $d_1 = 0.518$ nm and $d_2 = 0.302$ nm. The photograph inset in Figure 2 confirms that there were only two equatorial peaks.

The exact values of d_1 and d_2 depend on the draw ratio. Both d_1 and d_2 decrease with increasing draw ratio but the important feature is that the ratio $d_1:d_2$ always remains close to $\sqrt{3}:1$. The other effect of increasing draw ratio is that the arc width of the equatorial peaks decreases, reflecting the increasing orientation. Apart from this, the drawn, cast films always produced a pattern of the same general appearance as that in Figure 2, no matter what the molecular weight or the draw ratio.

The peaks in Figure 2, which are in the ratio $\sqrt{3}:1$, have been attributed to a hexagonal packing of rod-like PAN chains by Natta *et al.*²⁰ and other investigators¹⁷⁻¹⁹. According to Bohn *et al.*¹⁷, the PAN chain adopts a rod-like structure and these rods are able to pack with sufficient lateral order to produce the two equatorial peaks. The absence of any sharp non-equatorial peaks is attributed to the lack of chain-axis order¹⁷.

The diffractogram and the diffraction pattern of oriented PAN shown in Figure 2 have been reported not only by Natta *et al.*²⁰ but by Houtz¹⁶, Bohn *et al.*¹⁷, Statton¹⁸ and others^{19,21,22}. Similar diffractograms of unoriented PAN powder have been shown by Gupta and Chand²³, Sokoł and Turska²⁴ and others^{25,26}. Despite all efforts in the present work, with the uniaxially drawn films, we were unable to obtain the diffraction pattern found by Colvin and Storr¹², which remarkably showed two fairly intense and sharp meridional peaks with spacings of 0.354 and 0.177 nm.

Compression-elongated samples

The second type of sample in this work was made by a non-solvent based processing route. The compression-elongated strands could be elongated up to a maximum

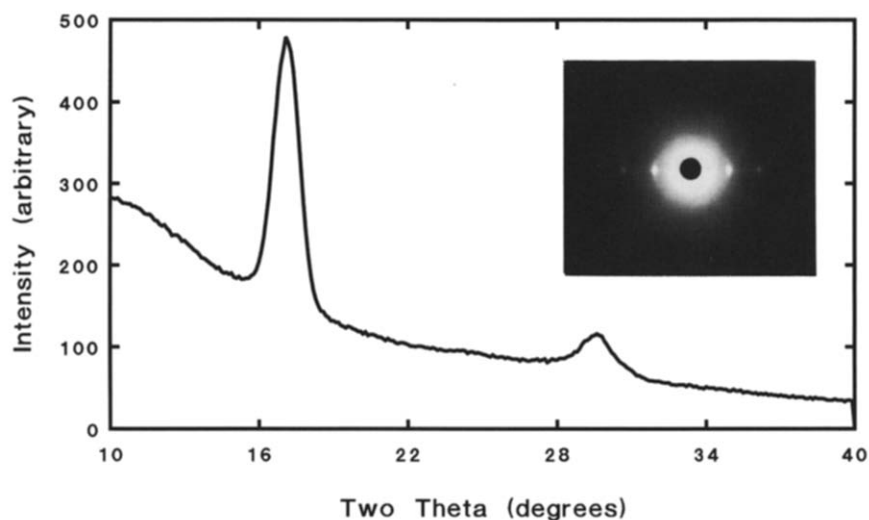


Figure 2 Equatorial diffractogram of a drawn, cast film showing the two peaks characteristic of the hexagonal polymorph. Inset shows the photographic diffraction pattern. Draw axis is vertical

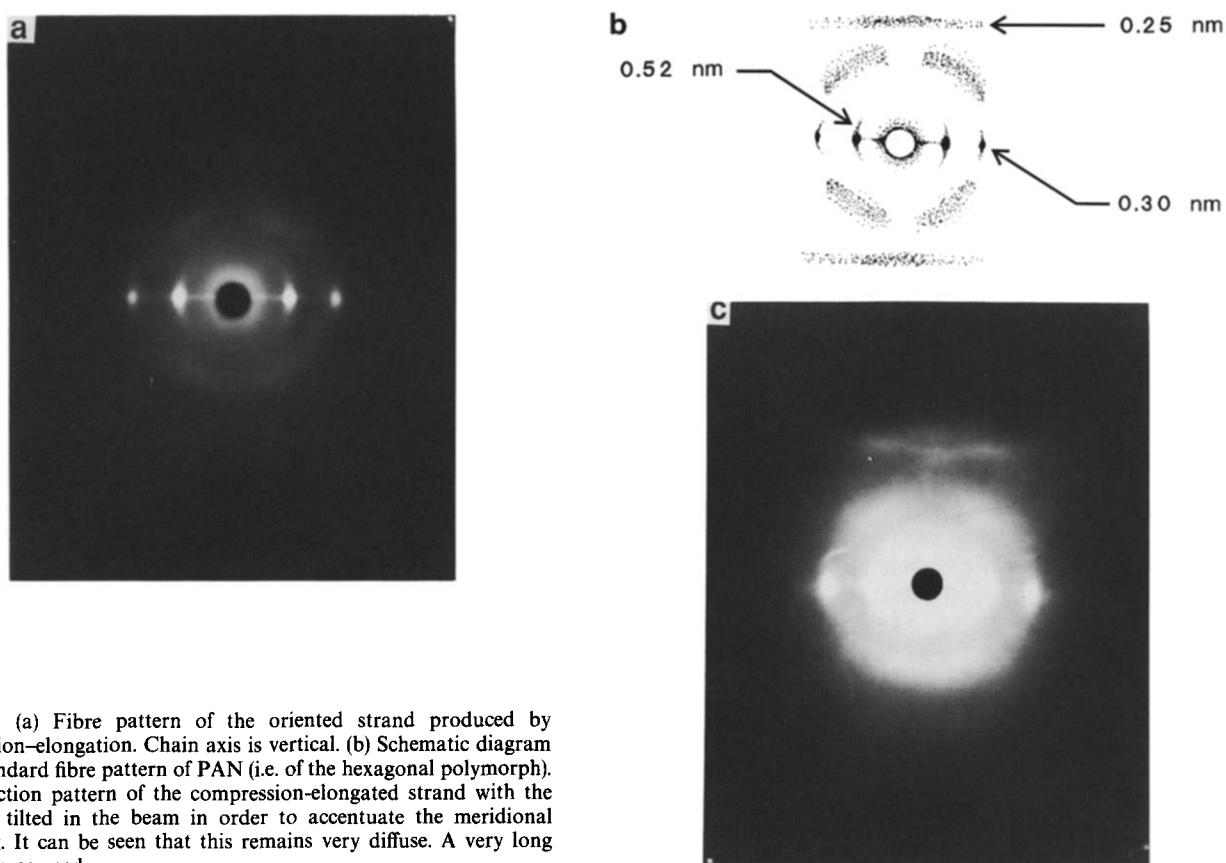


Figure 3 (a) Fibre pattern of the oriented strand produced by compression-elongation. Chain axis is vertical. (b) Schematic diagram of the standard fibre pattern of PAN (i.e. of the hexagonal polymorph). (c) Diffraction pattern of the compression-elongated strand with the specimen tilted in the beam in order to accentuate the meridional scattering. It can be seen that this remains very diffuse. A very long exposure was used

draw ratio of 19:1. Above this value, the sample was liable to tear. Although the polymer was exposed to a temperature of 135°C for a period of up to 3 h during the various processing cycles, no perceptible change due to thermal degradation was observed. The strands were transparent with a light tan colour. These highly oriented specimens were prone to splitting along the fibre axis.

Equatorial and meridional scattering. Figure 3a shows a fibre pattern of a strand with a draw ratio of 19:1 taken

with the X-ray beam perpendicular to the fibre axis. It can be seen that this is the conventional fibre pattern of the hexagonal polymorph and is the same as that observed with the drawn films in the previous section (Figure 2), and those reported by many workers^{16-18,22}. As with the drawn films, the limited arcing of the equatorial peaks signifies a high degree of orientation in the strand. The horizontal streak along the equator is due to the white radiation that was not removed by the Ni filter and is commonly observed in fibre patterns where

additional precautions have not been taken to monochromatize the beam²⁷.

In *Figure 3a*, there are two equatorial peaks, with spacings of 0.525 and 0.305 nm. These were also confirmed independently with an equatorial scan on the diffractometer. It can be seen that these peaks are close to the ratio $\sqrt{3}:1$, and hence they are characteristic of hexagonal chain packing²⁰. In addition to the equatorial peaks, there are weak, diffuse lobes along the meridian and the quadrants. These are very faint and cannot be easily discerned in *Figure 3a*. *Figure 3b* is a sketch of the diffraction pattern shown in *Figure 3a*.

Certain authors also quote a *c*-axis dimension for the hexagonal unit cell^{28,29}; the original works are difficult to trace, but presumably it is based on the diffuse meridional streak shown in *Figure 3a* and *b*. On the other hand, others including Bohn *et al.*^{17,30} have stated that the meridional and off-axis scattering is too diffuse to regard as crystalline diffraction peaks. Hence, they and others adopt a model with two-dimensional lateral order¹⁷⁻¹⁹. In the previous section, the diffuse non-equatorial scattering was not in fact observed with the drawn films, most probably because the samples were very thin ($\sim 20 \mu\text{m}$).

Following the procedure of Colvin and Storr¹² for investigating the non-equatorial scattering, the oriented strand was tilted 20° relative to the X-ray beam in order to accentuate the meridional scattering. The diffraction pattern acquired from this experiment is shown in *Figure 3c*. Meridional and off-axis scattering is present as weak, diffuse layer-lines centred about $2\theta = 37^\circ$. A diffractometer scan along the meridian was obtained from a sample which was drawn four times. We employed a sample with a draw ratio of 4:1 instead of 19:1 for the meridional scan because this sample was thicker and therefore it was possible to obtain a higher signal-to-noise ratio and a diffractogram in a realistic time. This is shown in *Figure 4*; a broad two-component peak in the vicinity of $2\theta = 37^\circ$ appears to be present. The maximum intensity of the two-component peak in *Figure 4* corresponds to a spacing of 0.246 nm.

Double orientation and hexagonal symmetry. With the compression-elongated strands, it was also possible to

record the diffraction pattern after passing the beam parallel to the fibre axis. This is shown in *Figures 5a* and *b* (the two patterns are from the same specimen and the only difference is that two different camera distances were used in order to highlight relevant details). Interestingly, it turned out that these strands had a double (i.e. biaxial) orientation, as revealed by the arcing of the 0.525 and 0.305 nm peaks in *Figure 5*. It can be seen that there is hexagonal symmetry. Note also that the faint pattern close to the beam stop in *Figure 5a* is due to the white radiation²⁷ and its cause is similar to that of the equatorial streak in *Figure 3a*.

By locking the diffractometer detector at the position of the equatorial reflection corresponding to 0.525 nm ($2\theta = 16.88^\circ$) and rotating the sample, the Bragg planes are brought in and out of the diffracting condition. A plot of scattering intensity *versus* sample orientation obtained by such a method is given in *Figure 6*. The data have not been processed to reduce the effects of sample absorption and any slight misalignment of the sample in the beam. These account for the peaks being of unequal heights. The angular separation of the peaks is *exactly* 60° however, confirming the presence of hexagonal symmetry.

Hexagonal symmetry was observed by Kumamaru *et al.* in electron diffraction photos acquired from solution-grown single crystals of PAN with the beam passed parallel to the chain axis¹⁴. They remarked that the peaks fitted Natta's hexagonal unit cell²⁰. (Note, however, Kumamaru *et al.* showed in the same work an X-ray photo of a single-crystal mat which displayed a totally different diffraction pattern.) Diffraction patterns similar to *Figure 5* are also observed with the smectic B phase in molecular liquid crystals such as 4-*n*-butyloxybenzal-4'-*n*-octylaniline and again this has been attributed to a hexagonal packing of mesogenic molecules³¹. However, in these two examples^{14,31}, the arcs are closer to being spots whose angular separation is exactly 60° . Though *Figure 3a* shows that the degree of chain-axis orientation is high, *Figure 5* shows that the degree of orientation of the other crystallographic axes is low and coupled with the sample misalignment, it results in the peaks being smeared into wider arcs.

As far as we are aware, the diffraction pattern in

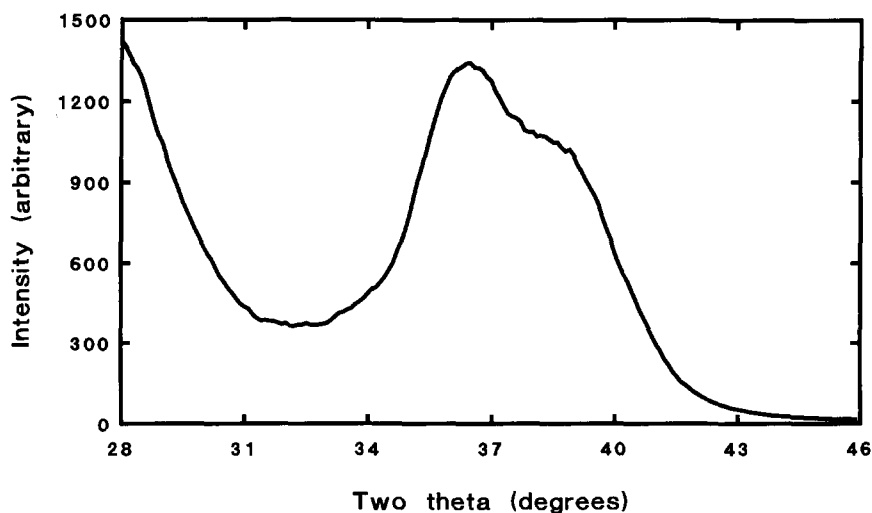


Figure 4 Meridional diffractogram of the compression-elongated specimen showing the presence of a broad, two-component peak

Figure 5 is the first direct evidence of hexagonal symmetry from a macroscopic sample of PAN. In all previous work with oriented fibres and films, the two equatorial peaks such as those in Figure 2, being in the ratio $\sqrt{3}:1$, were assumed to arise from a hexagonal lattice¹⁷⁻²⁰. Note that

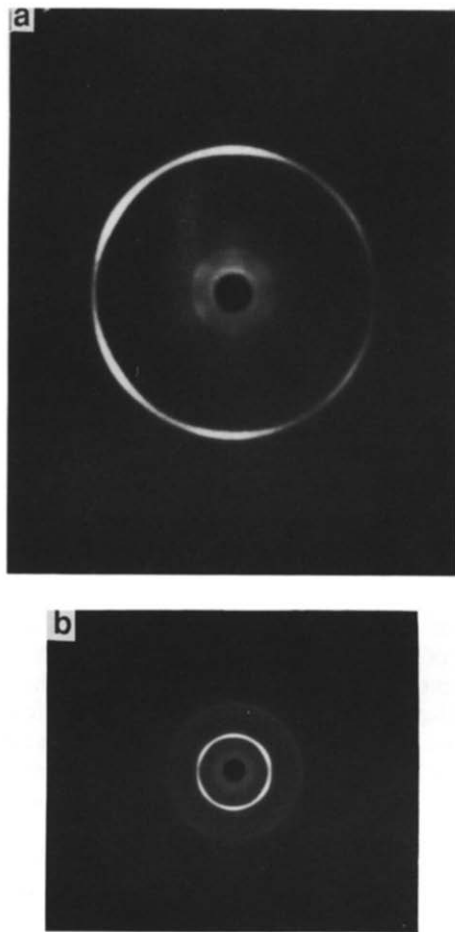


Figure 5 (a) Diffraction pattern of the compression-elongated PAN, with the X-ray beam passed down the axis of the oriented strand, shows the hexagonally symmetric arcing of the 0.525 nm spacing. (b) Diffraction pattern of the compression-elongated sample, with a different sample to film distance. The arcing of the fainter 0.305 nm (outer) peak can be seen. The inner peak is the 0.525 nm spacing, whose arcing can be seen better in (a)

if a similar experiment is attempted with a bundle of drawn fibres, with the beam passed down the fibre axis, the hexagonal arcing will not be observed, because fibres usually have uniaxial orientation.

The orientation of the diffraction pattern in Figure 5 with respect to the strand is shown in Figures 7a and b. The *c* (chain axis) direction is parallel to the fibre (elongation) axis and the *a*-axis of the unit cell must be parallel to the compression axis used to elongate the sample.

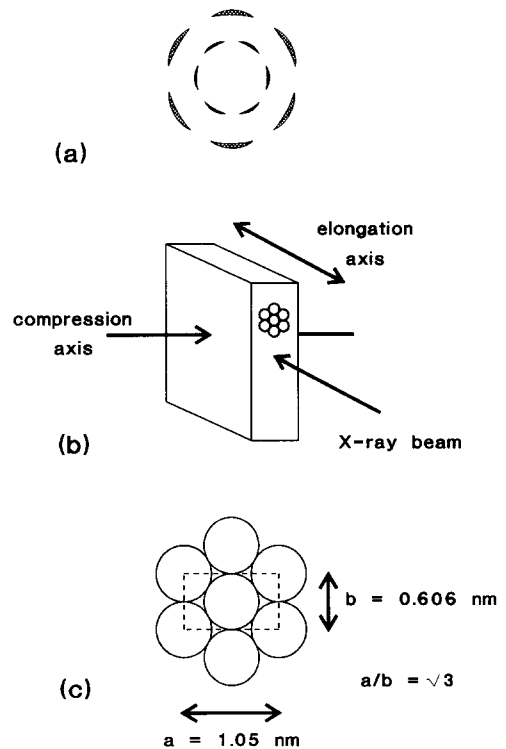


Figure 7 (a) Idealized hexagonal X-ray diffraction pattern. The inner set of arcs corresponds to the 0.525 nm spacing and the outer arcs to the 0.303 nm spacing. (b) Geometry of the compression-elongated sample with respect to the X-ray beam. The hexagonally packed circles represent the end-on view of the chains. (c) Hexagonal packing of rod-like PAN chains (cross-section) with rectangular unit cell. With this cell, $a/b = \sqrt{3}$ for hexagonal packing. The cell parameters depend on the degree of chain extension and those shown in the diagram are based on the *d*-spacings obtained from the compression-elongated strand

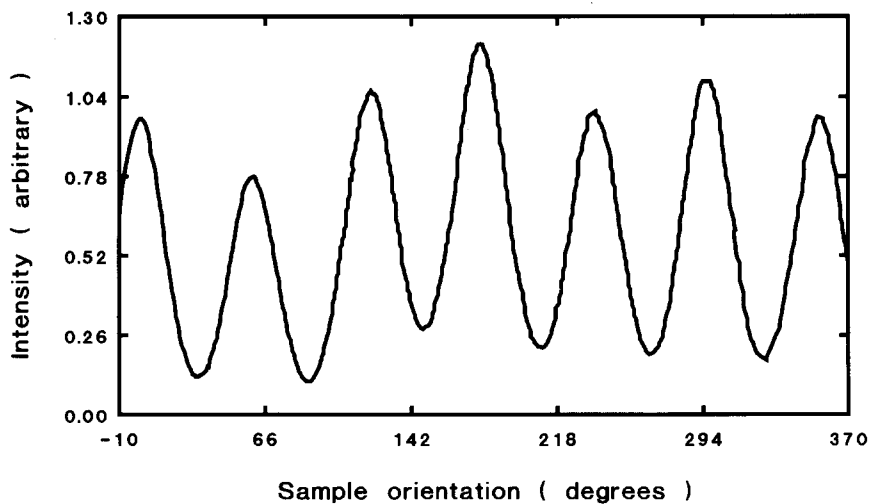


Figure 6 Variation of reflected X-ray intensity from compression-elongated PAN as it is rotated with the detector locked at $2\theta = 16.88^\circ$. The angular separation of the peaks is exactly 60°

In summary, with the compression-elongated sample as well as the drawn films, we were unable to find the meridional peaks reported by Colvin and Storr¹². Instead, we have found the 'standard' results quoted by many workers. Hexagonal packing has been explicitly dismissed by certain authors such as Menčík³², but our doubly oriented specimen strengthens the case for it.

Unit cell and density for the hexagonal polymorph

Even though the peaks in the standard diffraction pattern have been attributed to a hexagonal lattice, there is considerable discrepancy in the cell parameters cited for the hexagonal polymorph³³. It has been shown that with just two peaks, it is possible to index the hexagonal system in three ways³³. One possible choice is to use a pseudo-hexagonal (rectangular) cell to index the hexagonal lattice³³. We shall adopt such a cell here (Figure 7c).

For the compression-elongated sample, $d_1 = 0.525$ nm and $d_2 = 0.305$ nm. With these values of d_1 and d_2 , $a = 1.05$ nm, $b = 0.606$ nm and $a/b = \sqrt{3}$; this corresponds to the hexagonal packing of rods with a diameter of 0.606 nm (Figure 7c). Though Bohn *et al.*¹⁷ have dismissed the meridional scattering as too diffuse to regard as a crystalline peak, others^{28,29} appear to have adopted it to derive a c -value for the unit cell. Thus, if we take $c = 0.492$ nm from Figure 4, it is possible to calculate the crystal density (in g cm^{-3}) from:

$$\rho = (M_w \times 10^{-6} kn)/(abcN_A) \quad (1)$$

where $k =$ two chains per unit cell, $n =$ two repeat units per chain in the c -direction, $M_w = 53$ atomic mass units per repeat and $N_A = 6.02 \times 10^{23} \text{ mol}^{-1}$ (Avogadro's constant).

Substituting values for a , b and c given above for the compression-elongated sample yields 1.12 g cm^{-3} for the X-ray density.

For the drawn film in this work, the two peaks in Figure 2 give $d_1 = 0.518$ nm and $d_2 = 0.301$ nm. This can be indexed³³ using a pseudo-hexagonal cell with dimensions $a = 1.036$ nm, $b = 0.598$ nm and $a/b = \sqrt{3}$. It corresponds to the hexagonal packing of molecular rods with a smaller diameter of 0.598 nm (the rod diameter is equal to the b spacing and is given³³ in general by $2d_1/\sqrt{3}$). For the drawn films, it was not possible to acquire a meridional scan such as that in Figure 4 because with the extreme thinness of the film, the signal was too weak to record. However, if we adopt $c = 0.492$ nm (based on the diffuse meridional peak at 0.246 nm observed with the compression-elongated sample, Figure 4), a density of 1.155 g cm^{-3} is obtained. In a previous work, Bashir *et al.*³⁴ in fact obtained higher draw ratios with drawn, cast films which resulted in even smaller d -spacings ($d_1 = 0.509$ nm and $d_2 = 0.295$ nm). Using these values gives for the cell dimensions^{33,34} $a = 1.018$ nm, $b = 0.588$ nm and $a/b = \sqrt{3}$. Again adopting $c = 0.492$ nm and applying a similar calculation now gives a density of 1.196 g cm^{-3} . Thus, it seems that in samples with the higher orientation, higher X-ray densities are obtained due to the more efficient packing of chains.

The X-ray densities calculated above should be compared with density data measured by flotation in density-gradient columns. Even the latter data show considerable variation. According to the results reported by Rein³⁵ in 1949, the density of PAN lies between 1.17 g cm^{-3} and 1.22 g cm^{-3} . The density values cited by several other workers also lie in this range³⁶. Hurley and

Tzentsis³⁷ claimed to have obtained a density as high as 1.2323 g cm^{-3} in a freshly coagulated filament of the polymer; drawing apparently reduced the density to values between 1.1769 g cm^{-3} and 1.2257 g cm^{-3} . Menčík³² mentions that the experimentally measured densities for an unoriented polymer film and for a powder were 1.16 and 1.18 g cm^{-3} , respectively. Thus, the X-ray densities of 1.155 g cm^{-3} for the drawn film in this work and 1.196 g cm^{-3} for the oriented film from the previous work^{33,34}, compare favourably with the bulk densities measured by flotation columns and hence lend support to the hexagonal model for chain packing. The density value obtained from the compression-elongated sample is however, slightly on the low side.

Menčík cites the low value of the X-ray density he calculated (1.13 g cm^{-3}) as one of the reasons for dismissing hexagonal packing³². However, a variable density between $\sim 1.10 \text{ g cm}^{-3}$ and 1.20 g cm^{-3} can be obtained with the hexagonal model due to several reasons. First, the two d -spacings are dependent on the draw ratio^{33,34} and to obtain the highest density, samples with the highest degree of ordering must be used. More importantly, there is also a substantial degree of imprecision in the c -value because of the extreme weakness and diffuseness of the meridional peak, and small changes in this affect the density. The early workers^{27,28} report $c = 0.50$ nm, which implies that they measured the maximum of the diffuse meridional to be at 0.250 nm instead of 0.246 nm as found here. Apart from the experimental uncertainties cited above for the apparent density discrepancy, alternatively Liu and Ruland³⁸, who have conducted modelling studies based on hexagonal packing, suggested that the difference between the X-ray and the experimental density can be explained by assuming one kink per 10 monomer units.

When discussing the hexagonal model, Menčík³² did not recognize the possibility that the cell parameters depend on the draw ratio. In his review of the hexagonal model, Menčík used the following parameters (presumably taken from the literature of the period): $a = b = 0.6$ nm, $\gamma = 120^\circ$, $c = 0.5$ nm (hexagonal cell). Transforming to the equivalent pseudo-hexagonal cell gives $a = 1.04$ nm, $b = 0.60$ nm, $c = 0.50$ nm and $a/b = \sqrt{3}$. The density calculated from equation (1) then becomes 1.13 g cm^{-3} , which he concluded was too low and on this basis he ruled out the hexagonal model. (Menčík went on to derive an extraordinary orthorhombic cell which however, has not been reproduced by anyone³².) The values for the cell parameters of the compression-elongated sample in this work are similar to the one cited by Menčík for the hexagonal case, and hence the density of 1.12 g cm^{-3} for this sample is also similarly low. It appears that the compression-elongated samples were less ordered than the highly drawn films; this may have arisen because these samples were prepared at elevated temperatures and could only be cooled slowly after deformation.

Inspection of the diffraction patterns in Figures 3a and c shows that the meridional scattering is indeed very diffuse and Bohn *et al.*¹⁷ as well as Lindenmeyer and Hosemann³⁰ have cause to state that these cannot be regarded as crystalline peaks. Nevertheless, we have gone through the exercise of calculating a density using a value of the c -spacing obtained from such a diffuse meridional peak, solely to show that it does not rule out the hexagonal model as claimed by Menčík. An X-ray density close to 1.20 g cm^{-3} can be obtained when it is realized

that the values of a and b depend on the sample and that there is some indeterminacy in the value of c .

Estimate of the maximum modulus

We are convinced (after examining many specimens) that the diffraction pattern of dry PAN contains only two strong equatorial peaks, and the meridional scattering though present, is relatively weak and very diffuse; thus, the method of measuring the X-ray crystal modulus shown by Sakurada¹ for several semicrystalline polymers cannot be extended in a straightforward manner to PAN.

Despite this, we may still estimate the limiting modulus of PAN by a comparison with other linear polymers where the X-ray crystal modulus has been measured. Sakurada and Kaji³⁹ listed the ' f value', which is the force required to extend a polymer chain by 1%, for 25 well known polymers, not including PAN. The f values were calculated from experimental X-ray moduli of the polymers and the cross-sectional areas of the chains. According to them, in most cases, the f value is mainly dependent on the conformation adopted by the chains in the crystal and is almost independent of the side groups. Working in reverse, if the cross-sectional area and the conformation adopted by the chain are known, the expected f value associated with the conformation can be used to calculate the chain modulus.

The f values for a selected number of polymers from Sakurada and Kaji's list³⁹ are given in Table 1. It can be seen that polymers that adopt the all-*trans* (T type) conformations such as PE and poly(vinyl alcohol) have the highest f values as well as the smallest cross-sectional areas, and hence the highest chain moduli. Polymers that adopt a helical conformation generally have lower moduli. Thus, isotactic polypropylene and isotactic polystyrene (TG type) have lower f values of 1.2×10^{-10} and 0.81×10^{-10} N, respectively; these chains also have larger cross-sections (Table 1).

The best conformational picture of the PAN chain is given in the paper by Bohn *et al.*¹⁷. The atactic PAN chain cannot adopt an all-*trans* conformation but forms a randomly kinked, but semi-rigid structure, due to the intramolecular repulsions of the nitrile dipoles. Thus, the PAN chain behaves like a molecular rod. These rods have a diameter of ~ 0.6 nm and pack together hexagonally with no periodicity in the chain-axis direction.

With the model of the randomly kinked atactic chain, clearly, PAN cannot be expected to have the modulus of

type T polymers such as all-extended PE. However, it is not obvious how to apply the f values of polymers that adopt a contracted conformation, as the atactic nature of the PAN produced by free-radical polymerization⁴⁰ means that the chain does not adopt a regular helical conformation with a fixed pitch and handedness, unlike the case of (for instance) isotactic polypropylene and all the polymers considered by Sakurada and Kaji³⁹. However, the $TGT\bar{G}$ type of polymers such as α poly(vinylidene fluoride) (PVDF) and poly(vinylidene chloride) appear to have some conformational similarity to PAN and moreover have similar cross-sectional areas. Thus, if the f value of 1.5×10^{-10} N for a α PVDF from Table 1 is adopted for PAN, and the cross-sectional area A is computed from the radius R of the molecular rod [for the compression-elongated sample, from Figure 7c, $A = \pi R^2 = \pi(0.303 \times 10^{-9})^2 = 2.88 \times 10^{-19}$ m²], the chain modulus for PAN would be given by $E = (f/A)/0.01 = 52$ GPa. For the drawn film of this work, the rod radius and area were slightly smaller (0.299 nm and 2.81×10^{-19} m², respectively), and using this gives a value of 53 GPa. Using the data for the drawn films of a previous work³⁴, the rod radius and area were 0.294 nm and 2.81×10^{-19} m², respectively, and this gives a modulus of 55 GPa.

The value of 52–55 GPa appears to be a reasonable estimate for PAN. One would expect the maximum modulus to be much lower than PE, but a little higher than isotactic polypropylene. The highest reported moduli in oriented fibres and films of PAN are in the range of 30–33 GPa and thus the maximum modulus has to be higher than this.

While high molecular weight PAN generally gives fibres with higher moduli and strengths than the normal molecular weights used in fibre spinning, it would appear that PAN with ultra high modulus cannot be made by 'gel spinning' or by any other means, due to the intrinsic chain properties described above. Unlike a polymer such as PE, where fibres or films prepared from high molecular weight (low concentration) polymer solutions can be drawn over one hundred times, films cast from dilute solutions of ultra high molecular weight PAN cannot be drawn beyond twenty to thirty times because they invariably splinter. It is the intramolecular nitrile repulsions which cause the PAN chain to adopt a rod-like semi-extended conformation, but it is the same feature that does not allow the chain to unravel completely from its semi-extended conformation.

Table 1 f values, cross-sectional areas (A) of chains and X-ray crystal moduli (E) of polymers

Polymer ^a	Conformation ^b	f ($\times 10^{10}$ N)	A ($\times 10^{19}$ m ²)	E (GPa)	Ref.
PE	T	4.3	1.82	240	39
PVAL	T	5.4	2.16	255	39
α PVDF	$TGT\bar{G}$	1.5	2.58	60	39
PVDC	$TGT\bar{G}$	1.4	3.51	42	39
iPP	TG	1.2	3.44	42	9
iPS	TG	0.81	6.92	12	39
POM	G	0.91	1.72	54	39
PAN	–	(1.5)	2.88	(55)	–

^a PE, polyethylene; PVAL, poly(vinyl alcohol); α PVDF, poly(vinylidene fluoride), alpha polymorph; PVDC, poly(vinylidene chloride); iPP, isotactic polypropylene; iPS, isotactic polystyrene; POM, polyoxymethylene; PAN, polyacrylonitrile

^b T , *trans*; G , *gauche*; \bar{G} , *minus gauche*

Comparison with diffraction patterns in the literature

A peripheral question that remains to be answered is why we have not been able to observe the diffraction patterns of Colvin and Storr¹², or other authors who cite meridional peaks such as Hinrichsen and Orth¹³.

It has been mentioned that most investigators have found the diffractogram or the associated diffraction pattern of the type shown in Figure 2^{16-26,28,29}. It has, however, been shown that in solvent-containing gels of PAN, a diffraction pattern that is completely different from the hexagonal pattern is obtained^{26,41}. Importantly, it was found that the removal of the solvent caused a return to the standard hexagonal pattern^{33,42}. It was postulated that in the presence of solvent, solvated crystallites were formed and hence a new diffraction pattern was found^{19,33,41}. Sokoł *et al.*^{24,43,44}, who studied the swelling of PAN with polar organic solvents, found that the initial polymer had the diffractogram of the hexagonal polymorph, but after swelling, the diffractogram of the orthorhombic modification was obtained. Though they did not go so far as to suggest the formation of solvated crystallites, they did note that the effect was reversible; that is, on solvent removal, the hexagonal diffractogram was again obtained. Recently, Kim and Cho²¹ have reported that a PAN film cast from DMF and drawn seven times gives a diffraction pattern similar to that shown in Figure 2 or Figure 3a. When this film was swollen in an aqueous iodine/potassium iodide solution, a new set of peaks (including a 0.31 nm meridional spacing) was found. When the film was deiodinated (by extraction with acetone), the original diffraction pattern of the hexagonal polymorph was obtained. Kim and Cho's results²¹ also reinforce the suggestion made by Bashir that the 'non-standard' diffraction patterns are generally associated with the presence of solvent³³. Conversely, the results of this paper support the proposal that the hexagonal pattern is always associated with solvent-free polymer³³.

On starting this work, it was not realized that the diffraction pattern of PAN may be specimen-dependent. Thus we did not prepare the oriented samples in the same way as Colvin and Storr¹². Their samples were made by a solvent-based preparative route, which involved wet-spinning filaments from aqueous sodium thiocyanate solution. Hence, it may be that residual solvent was left in their fibre, so that they obtained a non-standard diffraction pattern. As we did not have facilities for wet-spinning fibres from sodium thiocyanate solution, we prepared drawn specimens from gel films made with aqueous sodium thiocyanate as solvent, in an effort to match as closely as possible their method of specimen production. The technique for making gel films was developed previously with organic solvents and involves infiltrating the aqueous sodium thiocyanate into the polymer powder and then compression moulding²⁶. Preliminary results show that the PAN-thiocyanate gels show extra peaks (i.e. a pattern different from that of the hexagonal polymorph), as reported by Bashir with organic solvents^{26,41}. However, even in these PAN-thiocyanate gels, the set of peaks reported by Colvin and Storr¹² was not found.

CONCLUSIONS

The original purpose of this work was to examine the possibility of using X-ray methods to measure the 'crystal

modulus' of PAN, based on examining the displacement of meridional spacings on the application of a stress. Though many reports in the literature state that PAN is an unusual polymer in that no sharp meridional peaks are present, certain authors such as Colvin and Storr¹², have displayed diffraction patterns with quite intense and sharp meridional peaks.

In this work, we used two types of oriented PAN. The first was a uniaxially oriented sample produced by drawing cast films. These displayed the standard hexagonal pattern with just two equatorial peaks. Meridional peaks were not visible even with sample tilting.

The second sample was a thick strand produced by a non-solvent based method which we have called 'compression-elongation'. This sample also showed the standard fibre pattern for PAN. That is, two equatorial spacings with the ratio $\sqrt{3}:1$ were found, just as with the drawn films. However, with this thicker sample, meridional scattering was detected but it was very diffuse and weak. Again, this was similar to the results reported by Bohn *et al.*¹⁷ from drawn PAN fibres prepared by wet spinning. The relatively sharp meridional peaks of Colvin and Storr¹² were not found, even after tilting this specimen in the beam.

Interestingly, the compression-elongated sample turned out to have double (biaxial) orientation. This was found when the X-ray beam was passed down the fibre axis. The diffraction pattern obtained in this experiment confirmed the presence of hexagonal symmetry, which is normally assumed in the interpretation of the standard fibre pattern.

The density calculations were not inconsistent with the hexagonal model either. The reason for the slight variation in density found when using the hexagonal model is because the lattice parameters *a* and *b* depend slightly on the degree of chain extension, and because there is imprecision in the *c* parameter due to the broadness and diffuseness of the meridional scattering (in fact, certain authors do not regard the meridional scattering as crystalline peaks).

Though we were unable to measure the X-ray modulus of PAN in the same way reported for other semicrystalline polymers due to the absence of sharp meridional peaks, by knowing that the PAN chain adopts a randomly kinked conformation, and comparing this with polymers that adopt a helical conformation, we have estimated that the maximum modulus would be about 55 GPa. In any case, we do not think that ultra high modulus can be obtained from *atactic* PAN.

It has been suggested previously that dry PAN (dry powder, drawn films and fibres) will always contain two equatorial peaks consistent with the hexagonal polymorph³³. The samples in this work support this postulate. On the other hand, solvent-containing gels give a different diffraction pattern^{26,41}. Thus, the standard diffraction pattern of PAN is that associated with the hexagonal polymorph while the non-standard patterns appear to have a link with the presence of solvent. In the case where a non-standard diffraction pattern has been cited in the literature^{12,13}, it is possible that unsuspected residual solvent may have had an influence.

REFERENCES

- 1 Sakaruda, I., Nukushina, Y. and Ito, T. *J. Polym. Sci.* 1962, **57**, 651

- 2 Shauffele, R. F. and Shimanouchi, T. *J. Chem. Phys.* 1967, **47**, 3605
- 3 Mizushima, S. and Shimanouchi, T. *J. Am. Chem. Soc.* 1949, **71**, 1320
- 4 Treloar, L. R. G. *Polymer* 1960, **1**, 95, 279 and 290
- 5 Shimanouchi, T., Asahina, M. and Enomoto, S. *J. Polym. Sci.* 1962, **59**, 93
- 6 Odajima, A. and Maeda, T. *J. Polym. Sci.* 1966, **C15**, 55
- 7 Hoogsteen, W., Kormelink, H., Eshuis, G., ten Brinke, G. and Pennings, A. J. *J. Mater. Sci.* 1988, **23**, 3467
- 8 Dulmage, W. J. and Contois, L. E. *J. Polym. Sci.* 1958, **28**, 275
- 9 Sakurada, I., Ito, T. and Nakamae, K. *Makromol. Chem.* 1964, **75**, 1
- 10 Dobretsov, S. L., Lomonosova, N. V., Stelmakh, V. P. and Frenkel, S. Ya. *Vsokomol. Soyed. SSSR* 1972, **A14**, 1143
- 11 Maslowski, E. and Urbanska, A. *America's Textile International, Fibre World, FW* 2 September, 1989
- 12 Colvin, B. G. and Storr, P. *Eur. Polym. J.* 1974, **10**, 337
- 13 Hinrichsen, G. and Orth, H. *Kolloid-Z. Polym.* 1971, **247**, 844
- 14 Kumamaru, F., Kajiyama, T. and Takayanagi, M. *J. Crystal Growth* 1980, **48**, 202
- 15 Stefani, R., Chevreton, M., Garnier, M. and Eyraud, C. *Comptes Rend.* 1960, **251**, 2174
- 16 Houtz, R. C. *Textile Res. J.* 1950, **20**, 786
- 17 Bohn, C. R., Schaeffgen, J. R. and Statton, W. O. *J. Polym. Sci.* 1961, **55**, 531
- 18 Statton, W. O. *Ann. NY Acad. Sci.* 1959, **83**, 27
- 19 Bashir, Z., Atureliya, S. K. and Church, S. P. *J. Mater. Sci.* 1993, **28**, 2721
- 20 Natta, G., Mazzanti, G. and Corradini, P. *Rendiconti delle sedute della Accademia Nazionale dei Lincei* 1958, **25**, 3
- 21 Kim, H. S. and Cho, H. H. *J. Appl. Polym. Sci.* 1993, **47**, 373
- 22 Mathur, R. B., Bahl, O. P. and Kundra, K. D. *J. Mater. Sci. Lett.* 1986, **5**, 757
- 23 Gupta, A. K. and Chand, N. *Eur. Polym. J.* 1979, **15**, 899
- 24 Sokoł, M. and Turska, E. *Acta Polym.* 1984, **35**, 135
- 25 Joh, Y. *J. Polym. Sci., Polym. Chem. Edn* 1979, **17**, 4051
- 26 Bashir, Z. *Polymer* 1992, **33**, 4304
- 27 Spruiell, J. E. and Clark, E. S. 'Methods of Experimental Physics' (Ed. R. A. Fava), Vol. 16, Academic Press, New York, 1980, p. 48
- 28 Urbanczyk, G. W. *Zeszyty Nauk, Politech. Lodz Wlokiennictwo* 1962, **9**, 79; *Chem. Abstr.* 1964, **61**, 5836(b)
- 29 Rein, H. in 'Landolt-Bornstein Tabellen' (Ed. W. Kast), Vol. 4, 6th Edn, Part 3, Springer-Verlag, Berlin, 1957
- 30 Lindenmeyer, P. H. and Hosemann, R. *J. Appl. Phys.* 1963, **34**, 42
- 31 de Vries, A. in 'Liquid Crystals, the Fourth State of Matter' (Ed. F. de Saeva), Marcel Dekker, New York, 1979, p. 7
- 32 Menčík, Z. *Vysokomol. Soyed.* 1960, **2**, 1635
- 33 Bashir, Z. *J. Polym. Sci., Polym. Phys. Edn* in press
- 34 Bashir, Z., Tipping, A. and Church, S. P. *Polym. Int.* 1994, **33**, 9
- 35 Rein, H. *Angew. Chem.* 1949, **61**, 242
- 36 Soedenyal, V. *Polym. Sci. USSR* 1960, **2**, 1635
- 37 Hurley, R. B. and Tzentsis, L. S. *J. Polym. Sci., Polym. Lett. Edn* 1963, **1**, 423
- 38 Liu, X. D. and Ruland, W. *Macromolecules* 1993, **26**, 3030
- 39 Sakurada, I. and Kaji, K. *J. Polym. Sci., Part C* 1970, **31**, 57
- 40 Bashir, Z., Manns, G., Service, D. M., Bott, D. C., Herbert, I. R., Ibbett, R. N. and Church, S. P. *Polymer* 1991, **32**, 1826
- 41 Bashir, Z., Church, S. P. and Price, D. M. *Acta Polym.* 1993, **44**, 211
- 42 Herbert, I. R., Tipping, A. and Bashir, Z. *J. Polym. Sci., Polym. Phys. Edn* 1993, **31**, 1459
- 43 Sokoł, M., Grobelny, J. and Turska, E. *Polymer* 1987, **28**, 843
- 44 Grobelny, J., Sokoł, M. and Turska, E. *Eur. Polym. J.* 1988, **24**, 1195